Short Communication

The Oxidation of Matrix Composite AlMg Reinforcement with SiC

S. Valdez[1,], J. Ascencio[1], S.R.Casolco[2], M.I.Pech-Canul[3]*

[1]Instituto de Ciencias Físicas-Universidad Nacional Autónoma de México, Av. Universidad S/N, Col. Chamilpa, 062210, Cuernavaca, Morelos, México
[2]Instituto Tecnológico y de Estudios Superiores de Monterrey-Vía Atlixcáyotl, 72800. Puebla, México.
[3]CINVESTAV-Saltillo, Carretera Saltillo-Monterrey Km13, Saltillo Coahuila, México
[*]E-mail: svaldez@fis.unam.mx

Metal matrix composite (MMC) are engineered materials manufactured by the action of incorporated reinforcement materials into metal matrix. As a result, stiff and hardened reinforcing phase in metallic matrix is obtained. The matrix includes non-ferrous structures; meanwhile reinforcing phases comprise hardened non-metallic particulates. The purpose of this paper is to investigate microstructural and electrochemical behavior of Al-Mg matrix reinforced with SiC particles. The Aluminum-Magnesium matrix composite was manufactured by the vortex method. SiC particles were mixed into steel tubes at 1500 rpm to molten Al-Mg as-cast alloy. The MMC was characterized with the purpose of studying chemical and electrochemical interactions of SiC particles with the metal-matrix. Results show that anodic dissolution in the cast Al-Mg matrix was accelerated by the formation of a non-stable oxide layer exhibiting partial protection with small resistance to polarization conditions, while the corrosion phenomena in Al-MMC was inhibited by the addition of silicon carbide particles.

1. INTRODUCTION

The aluminum MMC (Al-MMC) in as-cast state is considered for use in transportation vehicles due to their high specific strength, high specific Young's modulus, improved yield and creep strengths, elevated wear resistance and excellent properties at elevated temperature over conventional aluminum alloys [1]. The key to their properties improvement lies in the structure, chemistry and the nature of bonding of Al-SiC interfaces. Alloying elements such as Mg, SiC, Al_2O_3 which segregate at particle-matrix interfaces, have been found to improve the wettability [2,3]. In addition, SiC particles (SiCp)

can refine microstructure of Mg-Al alloys due to the formation of Mg_2Si and Al_2MgC_2 phases during solidification [4]. However, Al_2MgC_2 phase can react with water or water vapor leading a reaction product $MgAl_2O_4$. The SiC particles size in conjunction with magnesium content plays a fundamental role in the degree of modification of the aluminum matrix. The degree of modification or infiltration of SiCp increases with increase the magnesium content [5,6]. Furthermore, the degree of uniformity of SiC particles in the Al-alloy matrix improves increasing the SiC content, preferably when SiCp > 15 vol. % [7]. In particular, research aimed at the developed a new methodology of predicting realistic microstructures of aluminum alloy incorporating metal matrix composites such as SiC particles in which parameters such as average size, volume fraction and shape distribution of the aggregates directly affect the microstructural morphology [8]. It is well known that microstructures features are directly determined by their solidification process; internal structure of an alloy controls and modifies the nature and interaction type of the existing defects. In order to minimize internal defects during solidification, casting alloys are manufactured under pressure in a process called *squeeze casting* or *vortex technique* [9,10] which involves the incorporation of ceramic particles such as SiC into liquid aluminum melt producing well dispersed alloy [11]. This method is not expensive and easier compared to others process to prepare particulate MMCs [12], which solve problems of conventional solidification of wetting characteristics, sinking or floating behavior of particles, and viscosity of molten mixture. As a result, better mechanical properties can be achieved due to finer size of particulates with a size distribution in a wider range [13]. However, it should be born in mind that adequate incorporation of grain refinement into the Al-matrix with SiCp has restrictions with vortex technique because it depends of the nature of the grain refiner [14]. However, despite all these metallurgical characterizations, few works concerning the corrosion behavior of these alloys can be found like the research carried out by Arrabal et al., [15], where electrochemical characterization of Al-Mg alloys coated with thermal spray Al/SiCp composites is addressed. Because of SiC particles induce distinct phases along the Al-Mg matrix [5], it is expected to decrease corrosion resistance by the action of galvanic couple. The present investigation, therefore, aims to investigate the electrochemical response of aluminum MMC obtained by Vortex method incorporating SiC particles with Al-Mg matrix unreinforced alloy.

2. EXPERIMENTAL PROCEDURE

2.1 Synthesis of composites.

The unreinforced AlMg matrix was made in a resistance electrical furnace at 750°C, using a flux mixture of salts, in order to avoid contact with surroundings and preventing elements oxidation. The matrix alloy was re-cast and reinforced with 10 % SiC particles volume fraction. The particles were preheated at 870°C for 5 minutes. The particles reinforcement were incorporated by Vortex Method at 1150 rpm for 15 minutes.

2.2 Microstructural characterization.

Prior to microstructural characterization, samples were prepared by grinding on SiC metallographic paper from 240 to 1000-grit, polished with alumina (5.0 μm, 1.0 μm and 0.5 μm) cleaned in an ultrasonically bath and attacked with Keller reagent (HF, HCl and HNO₃) to reveal microstructure.

Samples were examined using scanning electron microscopy (SEM) Jeol 5900 equipped with an analyzer of Leica images and energy dispersive X-ray analyses (EDAX). X-ray diffraction was carried out using a filter of Nickel with CuKα radiation in Phillips diffractometer operated to 40kV. A composite sample was sectioned at superior, average and inferior part for its chemical and microstructural analysis. Chemical analyses were made by coupled plasma atomic emission spectroscopy using an Espectrolab spectrometer 5L. Table 1 displays the composite chemical composition. These results represent the average of five different analyses in three regions.

Table 1. Matrix alloy and Al-MMC (wt. %) composition determined by coupled plasma-atomic emission spectroscopy.

	Mg (wt. %)	Si (wt. %)	Al (wt. %)	Others (wt. %)
AlMg matrix	10		Bal	0.79
Al-MMC	8.71	10.70	Bal.	0.81

2.3 Electrochemical characterization.

Electrochemical test was carried out using a disc-shaped samples (0.5 in diameter) in a still solution of 3.5 wt.% NaCl.

Before immersion, specimens were ground to 1000-grit and then cleaned with deionized water followed by rinsing with ethanol and dried in a hot stream. Afterwards, specimens were exposed to the test solution for 1 to 28 days. After exposure, specimens were cleaned in 50 vol. % nitric acid (HNO₃) for 3 min as recommended by ASTM G31; finally, samples were carefully dried before weighting.

In order to estimate the corrosion rate by mass loss, gravimetric measurements were performed. The weight loss analysis were obtained from a weighed AlMgSiC composite for each immersion time during the first, second, third, fifth, seventh and twenty-eighth days.

The samples were weighed at times before and after to be introduced in 3.5 wt.% NaCl electrolyte. The corrosive sea water medium was mixed with a magnetic stirrer at room temperature and pH 5.6. These measurements were conducted on the surface material with 0.5 inches and the test were reproduced twice.

Potentiodynamic polarization measurements were also conducted on samples in a 3.5 wt.% NaCl solution in room temperature conditions. The applied potential was controlled using a

commercial potentiostat. The potentiodynamic polarization curves were carried out with 1.0 mV min^{-1} scan rate. The cathodic and anodic polarizations referred to E_{corr} were -1850 mV and 1550mV, respectively. The electrochemical cell was a three-electrode setup including the working electrode, a saturated calomel electrode and a graphite mesh as a counter electrode.
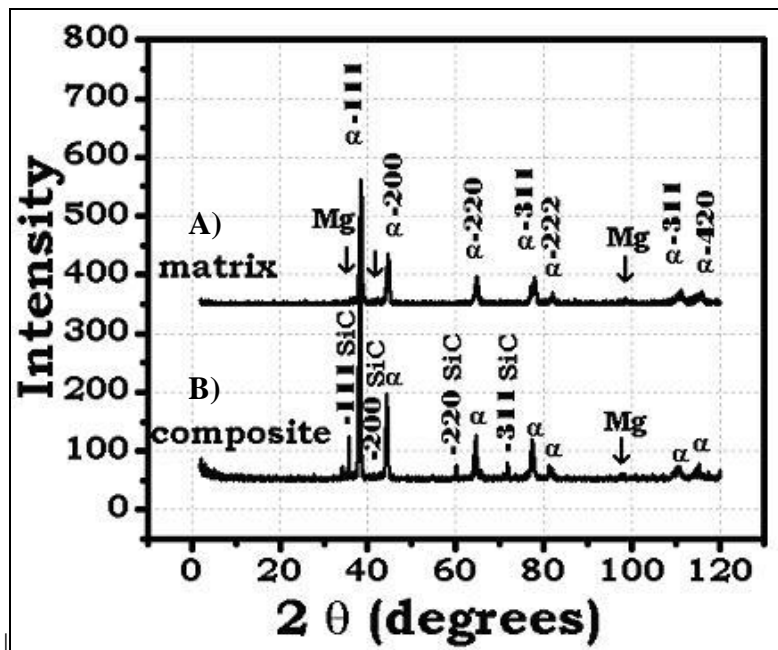
Figure 1. X-ray pattern showing the (A) α-aluminum and magnesium particles on the matrix alloy and (B) SiC particles in the Al-MMC.

3. RESULTS AND DISCUSSION

3.1 Materials and microstructure.

The XRD pattern from the Al-MMC manufactured by Vortex Method in conjunction with the matrix alloy (Figure 1) shows the diffraction intensity peaks corresponding to the α-aluminum phase, which is a solid solution rich in aluminum (α-Al) of crystalline structure FCC. The narrow peak detected for magnesium indicates low quantity of the element. Two main contributions can be identified: small peaks at 2θ − 38.82º and 2θ − 44.71º that corresponds to (111) and (200) reflection of α-Al phase, respectively.

On the other hand, the new composite show three main diffraction intensities: 2θ = 35.7º, 60.0º and 71.8º, which corresponds to (111), (220) and (311) of SiC particles, respectively. From diffractograms of Figure 1 it is feasibly to deduce the different crystalline phases of the master alloy and the composite material.

Table 2. Composition of Al-MMC and matrix alloy, (wt. %).

Phase	Elements			
	Al	Mg	Si	C
SS_{AlMg}	92.72	7.28	--	--
SS_{AlMg} + SiC	54.56	7.12	17.42	21.20
SiC			52.78	43.23

Several authors have studied the reactions between liquid aluminium in conjunction with reinforcement particles given by chemical reaction between Al matrix with the formation of intermetallic phases during processing [2]. Although, the case of Al-MMC manufactured with Vortex Method, does not induce further interactions during melting process, then, products of secondary reactions were not observed.

Table 2 shows the chemical analysis from the Al-MMC. Magnesium distribution has been entrapped into aluminum solid solution. Al-MMC did not show contributions of Si and C responsible of secondary chemical reactions.
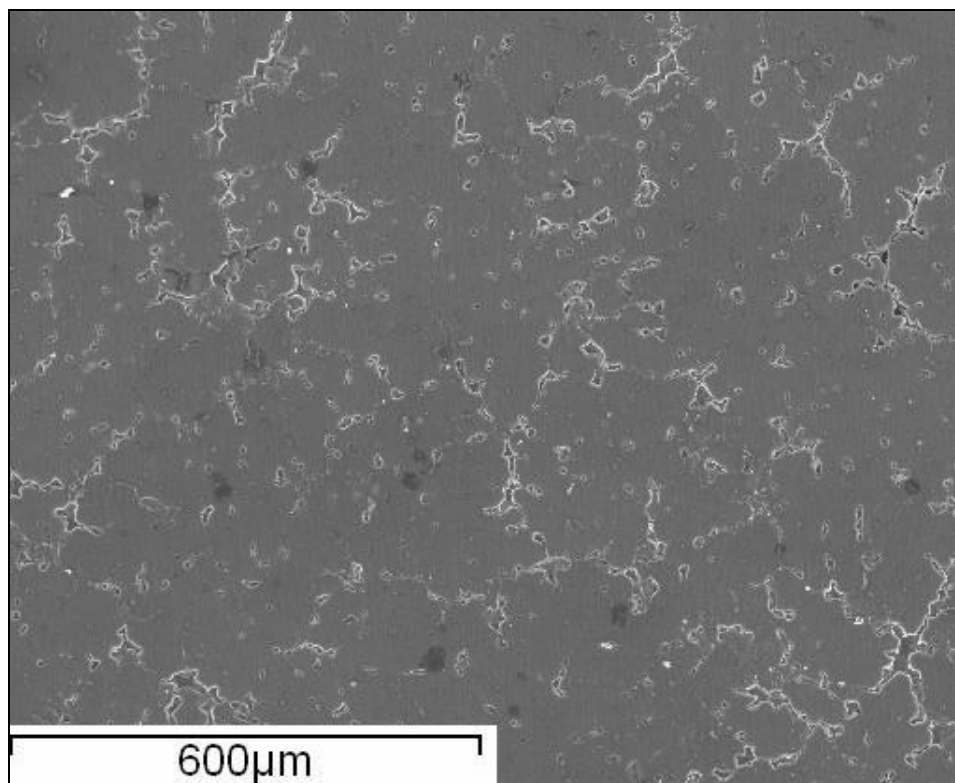

Figure 2. Matrix alloy microstructure constituted by Al-Mg solid solution rich in aluminum with dendritic microstructure.

Figure 2 and Figure 3 depicts morphology of master alloy (Al-Mg) and Al-MMC. Figure 2 shows the microstructure of master alloy, which was formed by Al-Mg solid solution (SS) rich in

aluminum with dendritic microstructure. Figure 3 shows the Al-MMC microstructure characteristic under as-cast condition with an EDAX spectrum from a spot of the solid solution. Nevertheless SiC particles does not suggest the presence of Al_2O_3 compound into the matrix as has been previously reported [8].


A

B
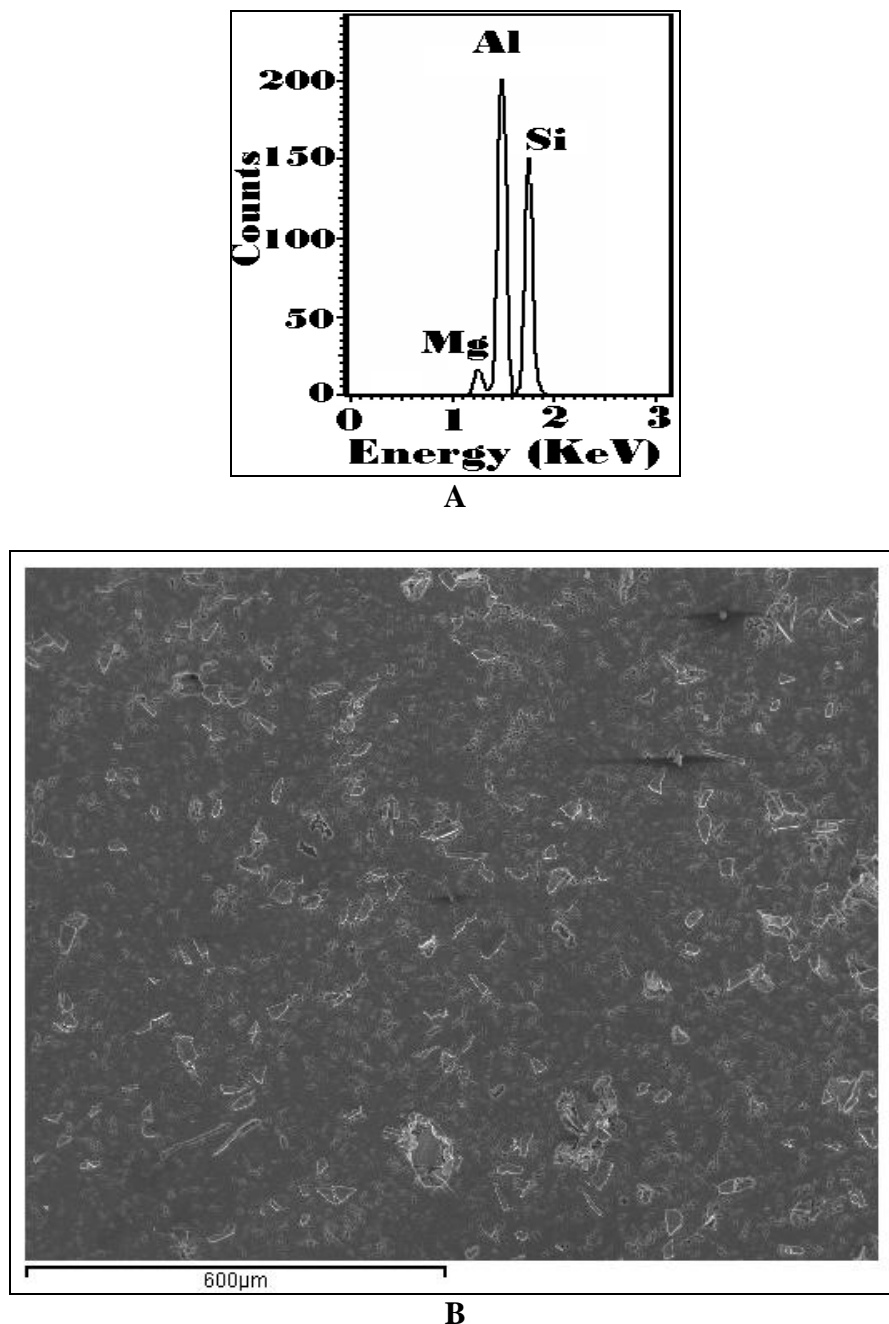
Figure 3. (A) Energy dispersive X-ray analyses spectrum from a spot of the solid solution interface with SiC particles. (B) Al-MMC microstructure of Al-Mg solid solution reinforcement with SiCp.

3.2. Electrochemical Characterization.

Polarization curves of Al-MMC and matrix samples carried out in 3.5 wt. % NaCl are shown in Figure 4. Former samples clearly show the effect of the SiC particles in the oxygen reduction reaction. At longer exposure times the limiting cathodic current became smaller. This behavior clearly shows that the SiC particles reduced the oxygen reduction rate approaching to a constant limiting current potential value under - 0.5 V (SCE). On the other hand, the anodic behavior indicates a constant increment in the anodic dissolution current at 24, 48 and 72 hours of immersion. From these potentiodynamic curves it can be observed that the anodic branch trend does not change in time achieving similar anodic currents along the test. Based on the polarization curves it can be state that the addition of SiC particles acts as a cathodic inhibitor reducing the availability of electrons for the cathodic reaction and therefore polarize the oxygen reduction reaction [16].

Concerning the master alloy measurements, the potentiodynamic behavior was different from the above results. The pattern of the polarization curves was approximately the same along the 72 hours of immersion. It clearly be seen that the cathodic curves achieved constant oxygen reduction rates as a consequence of a non-compact porous oxide film (Figure 4b). This behavior is confirmed in the anodic branch where an initial oxide layer originally formed at -0.71 V (SCE) was easily dissolved at higher anodic potentials indicating small resistance of the layer with poor adhesion properties to the anode. This phenomena lead to progressive anode dissolution. The nature of the film or passive film has been suggested as inert, thin and noncoherent formed on aluminium naturally which depend on alloy additions and contaminants [17].
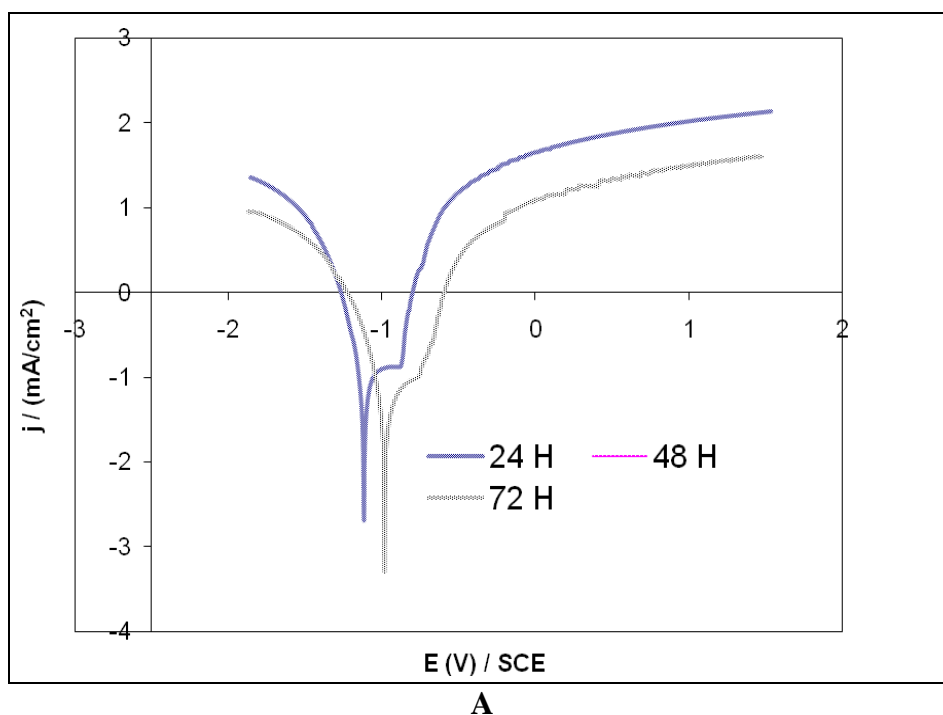
A
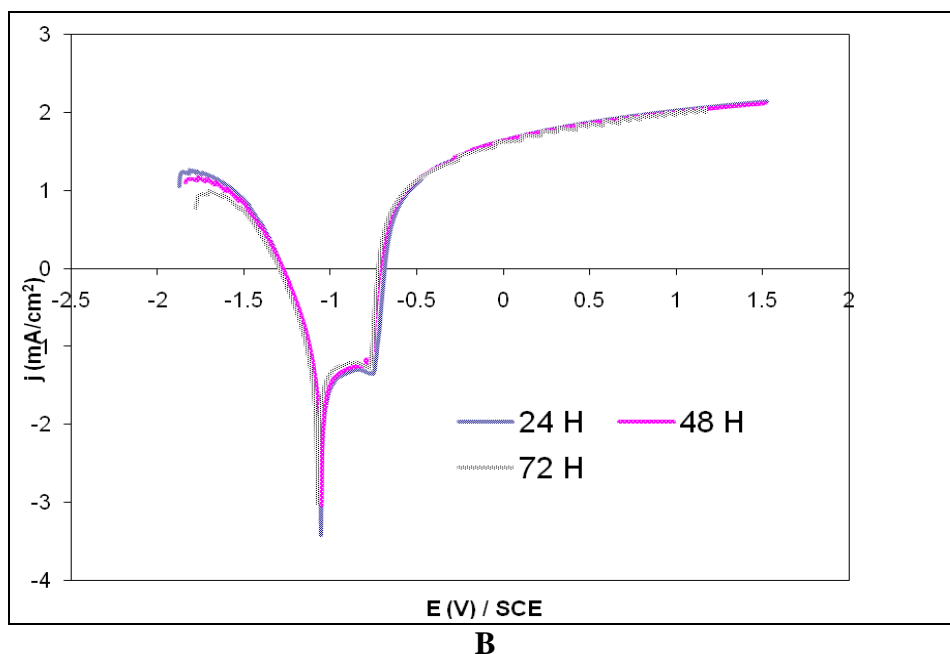
Figure 4. Polarization curves of a) Al-MMC, b) matrix alloy

The corrosion rate data of both, the Al-MMC and master alloys during 1800 h of immersion are summarized in Table 3. As can be observed, the effects of the addition of SiC particles are clearly appreciate between the two alloys. In contrast with the master alloy the corrosion rates of the modified alloy are lower at longer exposures times.

The corrosion rate was nearly four times lower than that achieved by the master alloy. This behavior could probably be ascribed to the fact that the aluminum solid solution did not exhibited precipitates of secondary phases as was already established by several authors [2]. It is generally accepted that secondary phases induce galvanic-couple mechanisms that activates anodes in contact with electrolyte in function of the precipitate composition [18], e.g. the anodic current increases when precipitates distribution reach a limit size within solid solution, leading small resistance to the oxide layer formed between boundaries grains permitting intense anode dissolution. This corrosion behavior, in the composite sample was not exhibited since no secondary chemical reaction was identified. The loss-weight data are qualitatively consistent with polarization curves of both samples.

Table 3. Corrosion rate of Al-MMC and matrix alloys during 1800 h of immersion.

Sample	Corrosion rate (mpy)	Standard Deviation
Al-MMC	0.17222	0.01189
Master alloy	0.6846	0.31287

According to the above results, it is estab0lished that a homogenous microstructure can be observed without particle agglomeration from the exterior to the interior of the sample. The addition of SiC particles can act either as solidification nuclei or SiC particles rejected towards grain boundary; these two phenomena mark differences in microstructural characteristics. Through Vortex Method agglomerates were not seen in the composites samples. SiC particles average size was 30μm homogenously distributed in both α-aluminum matrix and boundary grains (Figure 3). Homogenous distribution is the key to obtain better mechanical properties [19]. Many composite materials are used because of their high-specific elastic modulus, high-specific strength and good wear resistance. In addition the MMCs has been considered as potential lightweight and high-performance materials to be used in aerospace-craft, aircraft and engine parts in automobiles industry [20].

Advantages of the Vortex Method technique over conventional composite casting process are basically i) non-secondary chemical reaction with homogeneous particle distribution and ii) elimination of solidification defects due to the feeder tip system.

4. CONCLUSION

- Microstructural examination of Al-MMC manufactured under optimal conditions showed that distribution of particle reinforcement resulted homogeneous. Secondary chemical reactions were absent on the SiCp/matrix interface.
- Al-MMC alloy exhibited rich-aluminum Al-Mg solid solution.
- Corrosion phenomena in Al-MMC samples slowed down the oxygen reduction reaction; therefore, a decrement of the limiting cathodic current in function of time was achieved.
- The anodic dissolution of the matrix alloy was proved by the formation of a non-stable oxide layer exhibiting partial protection with small resistance to polarization conditions.
- The presence of Si in Al-Mg alloys did not lead an anode-like behavior with galvanic coupled characteristics.

References

1. A. Wlodarczyk-Fligier, LA. Dobrzanski, M.Kremzer, M.Adamiak; *J. Achiev. Mater. Manuf. Eng.* 27 (2008) 99.
2. M.Dyzia, J.Sleziona; *Arch. Mater. Sci. Eng.* 31 (2008) 17.
3. G.A. Kosnikov, O.L.Figovsky, a.S.Eldarkhanov; *Intern. Lett. Chem. Phys. Astron.* 6 (2014) 69.
4. Y. Huang, K. U. Kainer, N. Hort; *Scripta Mat.*, 64, 793 (2011).
5. Haris Rudianto, Yang Sang Sun, Kim Yong Jin, Nam Ki Woo; *Adv. Mater. Dev. Perform.* 6 (2012) 628.
6. A. Schiffl, M.A. Easton; *Mat. Sci. Forum* 445 (2009) 618.

7. Haris Rudianto, Sang-Sun Yang, Ki-Woo Nam, Yong-Jin Kim; *Rev. Adv. Mater. Sci*. 28. (2011) 34.
8. Riccardo Casati, Maurizio Vedani; *Metals* 4 (2014) 65.
9. K. Sukumaran, K.K. Ravikumar, S.G.K. Pillai, T.P.D. Rajan, M. Ravi, R.M. Pillai, B.C. Pai; *Mat. Sci. Eng* A., 490 (2008) 235.
10. T. Sornakrumar, M. Kathiresan; *Int. J. Miner. Metall. Mater,* 17(5) (2010) 648.
11. M. Kathiresan, T. Sornakumar; *Ind. Lubric. Trib*., 62(6) (2010) 361.
12. Yao Lei, Hao Hai, J. I. Shouhua, Fang Canfeng, Zhang Xingguo; *Trans. Nonferrous Met. Soc. China*. 21 (2011) 1241.
13. S. Sarkar, S. Mohan, S. C. Panigrahi; *J. Reinf. Plast. Comp*., 27(11), (2008) 1177.
14. S. Goussous, W. Xu, K. Xia; *J. Phys. Conf. Ser*. 240 (2010) 012106.
15. R. Arrabal, A. Pardo, M.C. Merino, M. Mohedano, P. Casajús, E. Matykina; *J. Therm. Spray Tech*., 20(3) (2011) 569.
16. R. Derakhshandeh, H.A. Jenabali Jahromi; *Mater. Design*. 32 (2011) 3377.
17. L. Zhang, D. G. Eskin, A. Miroux, L. Katgerman; *Light Metals* (2012) 999.
18. Q. Li, C.A. Rottmair; R.F. Singer; *Comp. Sci. Tech*. 70 (2010) 2242.
19. J.R. Gomes, A.S. Miranda, D. Solares, A.E. Dias, L.A. Rocha; *Ceram. Trans*. 114 (2000) 579.
20. J. Szajnar, M. Stawarz, T. Wróbel, W. Sebzda, *J. Achiev. Mater. Manuf. Eng*. 34(1) (2009) 95.